Crystallization Behaviour of *meso*-Λ(δλ)-[Co{*trans*-(*R*,*S*)(meen)$_2$}(C$_2$O$_4$)][Pb$_2$Cl$_5$]·2H$_2$O, Λ(λλ)-[{[Co{trans-(*R*,*R*)(meen)$_2$}(C$_2$O$_4$)]Br}$_2$]·3H$_2$O and *meso*-Δ(δλ)-[Co{*cis*-(*R*,*S*)(meen)$_2$}(C$_2$O$_4$)]I (meen = *N*-methylethylenediamine)†

Jiwen Cai, Jozef Myrczek and Ivan Bernal*
Department of Chemistry, University of Houston, Houston, Texas 77204-5641, USA

Proton NMR spectroscopy of a D$_2$O solution of the solid obtained by evaporating to dryness a reaction solution containing HCl, [Co(O$_2$CMe)$_2$]·4H$_2$O, PbO$_2$, H$_2$C$_2$O$_4$ and meen (meen = *N*-methylethylenediamine in water revealed the presence of two different isomers of the cation [Co(meen)$_2$(C$_2$O$_4$)]$^+$. Three isomers [Co(meen)$_2$(C$_2$O$_4$)][Pb$_2$Cl$_5$]·2H$_2$O **1**, [{[Co(meen)$_2$(C$_2$O$_4$)]Br}$_2$] **2** and [Co(meen)$_2$(C$_2$O$_4$)]I **3** were isolated eventually by the selective use of appropriate counter anions and their crystal structures determined. The ^{1}H NMR spectra of D$_2$O solutions of pure crystalline material from the same batch as that from which the structural crystals were derived showed the presence of single species of each of the three isolated compounds. Given their structures it is evident that the isomer with both methyls in the equatorial plane (*trans* to the oxalato oxygens) was either not formed or it rearranged soon after being formed. Complexes **1** and **2** are conformational isomers differing only in the relative position of one of the two axial methyl groups; **1** is stable in solution for at least 1 week at 21 °C, as demonstrated by its ^{1}H NMR spectrum and rearrangement of cation **2** to **1** and **3** takes several days. Compound **3** contains the expected axial–equatorial isomer.

It has been known for some time that [Co(en)$_2$(C$_2$O$_4$)]X (en = ethylenediamine X = Cl·4H$_2$O or Br·H$_2$O),[1-3] [Cr(en)$_2$(C$_2$O$_4$)]X (X = Cl or Br)[1,3] and [Rh(en)$_2$(C$_2$O$_4$)]Br[3] crystallize as conglomerates, but that [Co(en)$_2$(C$_2$O$_4$)]I crystallizes as both a conglomerate and a racemate.[2] We have recently determined[3] the crystal structures of the optically active forms of [Co(en)$_2$(C$_2$O$_4$)]X (X = Cl·4H$_2$O, Br·H$_2$O or I), their absolute configurations, conformations, and the similarities and differences in their crystal packing. These studies were carried out with crystals obtained from racemic solutions which crystallized as conglomerates.[4] At that time we pointed out that[4] the conglomerate crystallization of [Co(en)$_2$(C$_2$O$_4$)]X (X = Cl·4H$_2$O or Br·H$_2$O) is caused by the formation of spiral strings of cations held together by strong O · · · H$_2$N hydrogen bonds in which terminal oxalato oxygens bind three hydrogens of an adjacent cation giving rise to a three-point chiral recognition pattern connecting adjacent members of these spiral strings. Also that the stitching of spirals of the same, or of opposite, handedness is dependent on the counter ions and, where relevant, the waters of crystallization; the deciding factor is the strength of the hydrogen-bonding scheme which would result from joining spirals of the same or opposite chirality. Therefore, the observation by Yamanari and co-workers[2] that the chloride and bromide crystallize as conglomerates while the iodide crystallizes as both enantiomorphic and racemic crystals suggests that the weakness of the hydrogen bonds of the iodide results in little or no difference in the energetics of either scheme; thus, homo- or hetero-chiral strings are stitched equally well (or badly), and this may be the origin of the poor quality of the crystals one obtains with iodide.[4] Incidentally, similar observations of poor crystalline quality for related oxalato iodides were reported by Marusak *et al.*[5]

In view of the fact that the diastereoisomers we were interested in were unknown we thought it fascinating if they could be separated and characterized structurally to ascertain whether conformational and configurational changes in the cation result in changes in the enantiomorphic composition of the crystals and, thus, in the mode of packing of the resulting lattices; *e.g.* racemates *vs.* conglomerates and kryptoracemates.

The three geometrical isomeric cations of composition [Co(meen)$_2$(C$_2$O$_4$)]$^+$ (meen = *N*-methylethylenediamine) have two, three or four basal-plane amine hydrogens; consequently, the formation of spiral strings is still possible, as was the case with [Co(dmen)$_2$(C$_2$O$_4$)]I·2H$_2$O[5] (dmen = *N*,*N*′-dimethylethylenediamine) which has one hydrogen at each of the four amine nitrogens. Moreover, the stitching of the spiral strings into an enantiomorphic lattice by hydrogen bonds is also possible with a *N*,*N*′-dimethylated ligand having the appropriate conformation of the en rings. It is not possible with an axial–axial *N*,*N*-dimethylated ligand since the spiral strings can be formed but the interspiral linking hydrogens necessary would not be available. Thus, we decided to explore the crystallization behaviour of the monomethylated derivatives hoping to obtain cations with appropriate configurations and conformations.

Experimental

Syntheses.—The preparation and separation of the isomers involved synthetic and NMR procedures. Therefore, we incorporate in this section that portion of the NMR results without which we could not have carried out the syntheses and separations effectively. Other details of the NMR spectral study are described below.

As mentioned above, it was our intention to prepare [Co(meen)$_2$(C$_2$O$_4$)]Cl using the procedure of Jordan and Froebe[6] while substituting *N*-methylethylenediamine for ethylenediamine. The reaction solution was filtered to remove precipitated PbO and PbSO$_4$, evaporated to dryness in a rotary evaporator and recrystallized from deionized water. The first three crops of crystals isolated from this medium consisted of a small number of very well formed, red prisms which, initially, we took to be the desired product. The density and cell constants of these crystals indicated something considerably heavier than

---

† *Supplementary data available:* see Instructions for Authors, *J. Chem. Soc., Dalton Trans.*, 1995, Issue 1, pp. xxv–xxx.

oxalato chlorides had to be present. In view of these observations, we repeated the synthesis of Jordan and Froebe[6] and found that, indeed, one isolates in high yield the desired $[Co(en)_2(C_2O_4)]Cl{\cdot}4H_2O$, the structure of which we have reported elsewhere.[4] A microprobe analysis of the compound revealed the presence of Co, Pb and Cl in an approximate ratio of 1:2:5.*

After no further crystals of the complex $[Co(meen)_2(C_2O_4)][Pb_2Cl_5]{\cdot}2H_2O$ **1** had separated, the mother-liquor was once more evaporated to dryness, the solid redissolved in deionized water and the solution divided into two halves. One was treated with NH_4Br and the other with NaI. The crude solid obtained as a bromide proved to be a mixture of the bromides eventually characterized as an 85% enantiomorphic mixture of the ax-ax(*RR*)/(*SS*) isomers and 15% of the enantiomorphic pair present in **1**, as demonstrated by the ^1H NMR spectrum shown in Fig. 7(*b*). Recrystallization of the bromide mixture gave pure crystalline $[\{[Co(meen)_2(C_2O_4)]Br\}_2]{\cdot}3H_2O$ **2**, the ^1H NMR spectrum of which is shown in Fig. 8(*a*). This spectrum was obtained after warming a solution of crystals **2** in D_2O in order to accelerate the exchange of amino hydrogens.

The crude solid precipitated as the iodide is also a mixture of the cations present in complexes **1** and **2**. However, its composition [see Fig. 7(*c*)] consists of 80% of the enantiomorphic pair of ax-ax-Λ(*RR*)/Δ(*SS*) isomers present in **2**, and 20% of the enantiomorphic ax-ax-Λ(*RS*)/Δ(*SR*) pair present in **1**. Upon recrystallization of the solid iodide, pure ax-eq-Λ(*RS*)/Δ(*SR*) $[Co(meen)_2(C_2O_4)]I$ **3** was obtained, as shown by the elemental analysis and by its crystal structure which revealed that the recrystallization step was accompanied by isomerization. We believe this rearrangement of isomers was caused by photoactivation of the iodide (see below) which in turn causes the rearrangement. Consequently, the ^1H NMR spectrum of a solution of the crude iodide was recorded and after 7 d at 20 °C as shown in Fig. 9(*b*) and 9(*c*).

Elemental analyses were performed by Galbraith Laboratories, Knoxville, TN (Found: C, 10.20; H, 2.60; N, 6.05; Pb, 46.40. Calc. for $C_8H_{24}Cl_5CoN_4O_6Pb_2$: C 10.40; H 2.60; N; 6.05; Pb; 44.90. Found: C, 23.95; H, 5.75; N, 13.75. Calc. for $C_{16}H_{46}Br_2Co_2N_8O_{11}$: C, 23.90; H, 5.70; N; 13.95. Found: C, 22.55; H, 4.70; N, 13.85. Calc. for $C_8H_{20}CoIN_4O_4$; C, 22.75; H, 4.75; N, 13.30%).

X-Ray Diffraction:—Data were collected at 294 K with an Enraf-Nonius CAD-4 diffractometer operating with a Molecular Structure Corporation TEXRAY-230 modification of the SDP-Plus software package using Mo-Kα radiation (λ = 0.710 73 Å).[7] The raw data sets were processed either with this package or with the NRCVAX package (486/66 Mz personal computer version).[8] The crystals were centred with data in the $24 \leqslant 2\theta \leqslant 36°$ range and examination of the cell constants and Niggli matrix[9] clearly showed all three substances to crystallize in primitive, monoclinic lattices the systematic absences of which belong to those of the space groups $P2_1/n$, Pn and $P2_1/n$ for complexes **1**, **2** and **3**, respectively. The $F(hkl)_{obs}$ sets were corrected for absorption using empirical curves derived from ψ scans[7] of suitable reflections. The scattering curves were taken from Cromer and Waber's compilation.[10] The three structures were solved by the Patterson method and once the heavy-atom skeletons were found the hydrogen atoms of the cations were added at idealized positions (N–H = C–H 0.95 Å; B = 5.0 Å^2, fixed). The water hydrogens were found experimentally and fixed at these positions (B = 5.0 Å^2, fixed). The data for **1** and **3** were processed with the Nonius programs while those for **2** were processed with the personal computer version of the NRCVAX programs.[8] The weighting scheme used was $1/[\sigma(I)]^2$ throughout.

The complex *meso*-Λ(δλ)-$[Co\{trans\text{-}(R,S)(meen)_2\}(C_2O_4)][Pb_2Cl_5]{\cdot}2H_2O$ **1** crystallizes in space group $P2_1/n$ (no. 14), with lattice constants a = 10.532(2), b = 15.126(5), c = 14.564(3) Å, β = 109.10(2)°; U = 2192.44 Å^3 and D_c (M = 922.902, Z = 4) = 2.796 g cm^{-3}. 4991 Data were collected over the range of $4 \leqslant 2\theta \leqslant 50°$; of these, 2372 [independent and with $I \geqslant 3\sigma(I)$] were used in the structural analysis. Data were corrected for absorption (μ = 168.278 cm^{-1}) and the transmission coefficients ranged from 0.6662 to 0.9952; $F(000)$ = 1696. The final $R(F)$ and $R'(F)$ residuals were 0.0309 and 0.0389.

The complex Λ(λλ)-$[\{[Co\{trans\text{-}(R,R)(meen)_2\}(C_2O_4)]Br\}_2]{\cdot}3H_2O$ **2** crystallizes in space group Pn (no. 7), with a = 6.757(1), b = 17.474(1), c = 12.797(1) Å, β = 99.55(2)°; U = 1490.0(3) Å^3 and D_c (M = 803.24, Z = 4) = 1.790 g cm^{-3}. A total of 2736 data were collected over the range of $4 \leqslant 2\theta \leqslant 50°$; of these, 2318 [independent and with $I \geqslant 3\sigma(I)$] were used in the structural analysis. Data were corrected for absorption (μ = 30.8 cm^{-1}) and the transmission coefficients ranged from 0.5231 to 0.9978; $F(000)$ = 820. The final $R(F)$ and $R'(F)$ residuals were 0.047 and 0.060.

The complex *meso*-Δ(δλ)-$[Co\{cis\text{-}(R,S)(meen)_2\}(C_2O_4)]I$ **3** crystallizes in space group $P2_1/n$ (no. 14), with a = 12.795(4), b = 7.170(1), c = 16.733(10) Å, β = 109.12(3)°, U = 1450.40 Å^3 and D_c (M = 422.11, Z = 4) = 1.931 g cm^{-3}. A total of 1808 data were collected over the range of $4 \leqslant 2\theta \leqslant 45°$; of these, 1404 [independent and with $I \geqslant 3\sigma(I)$] were used in the structural analysis. Data were corrected for absorption (μ = 32.962 cm^{-1}) and the transmission coefficients ranged from 0.7476 to 0.9951; $F(000)$ = 832. The final $R(F)$ and $R'(F)$ residuals were, 0.0689 and 0.0828.

Additional material available from the Cambridge Crystallographic Data Centre comprises H-atom coordinates and thermal parameters.

Results

Crystallography.—In crystals of complex **1** the cations exist in the lattices as the enantiomeric pair *meso*-Λ(δλ)-$[Co\{trans\text{-}(R,S)(meen)_2\}(C_2O_4)][Pb_2Cl_5]{\cdot}2H_2O$ and *meso*-Δ(λδ)-$[Co\{trans\text{-}(S,R)(meen)_2\}(C_2O_4)][Pb_2Cl_5]{\cdot}2H_2O$, where *meso* refers to the fact that the two NH(Me) chiral centres are a mesomeric (*R*,*S*) pair located *trans* to each other and occupying the axial positions about the cobalt co-ordination sphere. Both methyls lie on the same side of the vector N(1)–N(4) [the two axial NH(Me) nitrogens]. The second compound, Λ(λλ)-$[\{[Co\{trans\text{-}(R,R)(meen)_2\}(C_2O_4)]Br\}_2]{\cdot}3H_2O$ **2** contains two cations in the asymmetric unit with chiroptical symbols Λ(λλ) or their enantiomorphs. In this case, *trans*-(*R*,*R*) means that the methylated nitrogens are an *R*,*R* pair located *trans* to each other and occupying the axial positions about the cobalt co-ordination sphere. The methyls lie on opposite sides of the vector N(1)–N(4) [the two axial NH(Me) nitrogens]. That is, the two cations differ from those in **1** by the chirality at one of the MeN nitrogens as well as the helical chirality of one of the en rings, which in **2** are in the highest-energy conformation; *e.g.* either Λ(λλ) or Δ(δδ). In both **1** and **2**, the equatorial plane is defined by the two oxalato oxygens and the two H_2N ligands.

In complex **3** the cations exist in the lattice as *meso*-Δ(δλ)-$[Co\{cis\text{-}(R,S)(meen)_2\}(C_2O_4)]^+$ and *meso*-Λ(λδ)-$[Co\{cis\text{-}(S,R)(meen)_2\}(C_2O_4)]^+$ pairs related to one another by the inversion centre of the space group. Final coordinates for **1**–**3** are listed in Tables 1–3. The structure of the cation present in **1** is shown in Fig. 1, and the contents of the asymmetric unit in **2** and **3** are shown in Figs. 2 and 3. The packing of the anions in **1** was shown in an early communication.[11] However, in that communication we did not show the packing of the cations and waters of crystallization which is therefore depicted in Fig. 4. The packing of the contents of the unit cells of **2** and **3** are shown in Figs. 5 and 6. Bond lengths, angles and selected hydrogen bonds are given in Tables 4–6 respectively.

---

* We thank Professor D. Elthon of this Department for the microprobe measurements.

Table 1 Positional parameters and their estimated standard deviations (e.s.d.s) for compound **1**

Atom	*x*	*y*	*z*
Pb(1)	−0.065 25(5)	0.352 01(4)	0.603 52(3)
Pb(2)	−0.030 35(5)	0.346 56(4)	0.879 84(3)
Cl(1)	0	0.5	0.5
Cl(2)	−0.321 6(4)	0.283 3(3)	0.489 3(3)
Cl(3)	−0.221 3(3)	0.432 8(2)	0.710 6(2)
Cl(4)	−0.067 7(4)	0.210 4(2)	0.732 9(3)
Cl(5)	0	0.5	1.0
Cl(6)	0.140 3(3)	0.412 8(2)	0.789 9(3)
Co	0.400 2(2)	0.277 4(1)	0.654 0(1)
O(1)	0.209 5(8)	0.293 3(6)	0.606 2(6)
O(2)	0.373 9(8)	0.223 1(6)	0.531 5(5)
O(3)	0.030 6(8)	0.261 1(6)	0.480 6(6)
O(4)	0.215 8(9)	0.197 2(6)	0.392 5(6)
N(1)	0.374(1)	0.162 1(7)	0.709 8(7)
N(2)	0.585 1(9)	0.248 5(7)	0.687 4(7)
N(3)	0.420(1)	0.340 2(7)	0.774 0(7)
N(4)	0.432(1)	0.394 5(7)	0.602 3(8)
C(1)	0.510(1)	0.124(1)	0.767(1)
C(2)	0.601(1)	0.151 3(9)	0.708 0(9)
C(3)	0.466(1)	0.432(1)	0.770(1)
C(4)	0.403(1)	0.463(1)	0.667(1)
C(5)	0.153(1)	0.262 4(8)	0.523 3(8)
C(6)	0.255(1)	0.224 0(9)	0.478 4(9)
C(7)	0.286(1)	0.154(1)	0.770(1)
C(8)	0.363(1)	0.414 3(9)	0.500(1)
O(w1)	0.153(1)	0.074 4(8)	0.553 9(9)
O(w2)	0.869(2)	0.096 (1)	0.533(1)

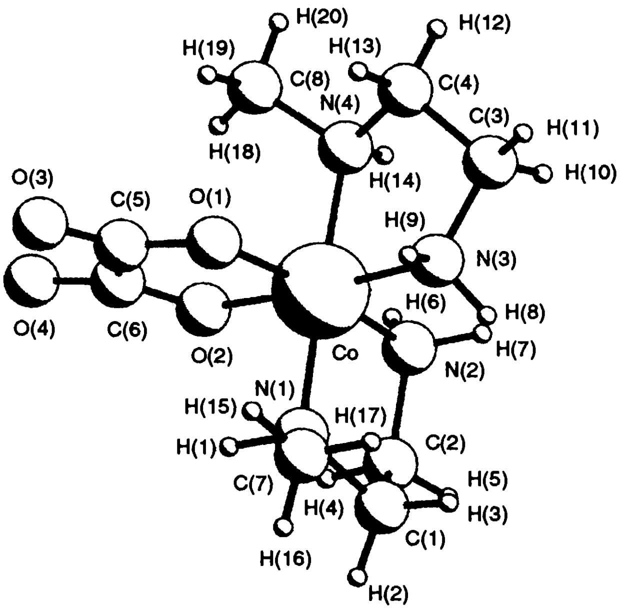

Fig. 1 Stereochemistry of the cations present in compound **1** with the numbering system

NMR Spectra.—Study of the NMR spectra of our compounds revealed rearrangements of isomers and their relative stabilities. These spectra are shown in Figs. 7–9. Fig. 7(*a*) shows that the efficient one-step reaction of Jordan and Froebe,[6] using meen instead of en, produced a mixture of two isomers as was verified by the X-ray crystallographic study of **1** and **2**, both of which contain methylated axial amine nitrogens (ax-ax isomers). If the product of the reaction is treated with an excess of bromide a solid is obtained which, when dissolved in D_2O, produces the NMR spectrum shown in Fig. 7(*b*). Likewise, precipitation of the crude product with iodide yields spectrum 7(*c*).

Table 2 Positional parameters and their e.s.d.s for compound **2**

Atom	*x*	*y*	*z*
Br(1)	0.321 42	0.294 41(12)	0.497 34
Br(2)	0.913 9(5)	0.274 53(15)	0.090 28(23)
Co(1)	0.819 4(5)	0.989 04(13)	0.424 69(24)
Co(2)	1.103 9(5)	0.501 27(15)	0.689 36(25)
O(1)	0.739 1(17)	1.013 3(7)	0.276 4(9)
O(2)	1.082 4(17)	0.978 1(7)	0.387 9(9)
O(3)	0.866 7(19)	1.031 4(8)	0.130 1(9)
O(4)	1.240 0(18)	0.990 7(8)	0.249 5(10)
O(5)	1.026 7(17)	0.527 1(8)	0.540 4(9)
O(6)	1.369 0(19)	0.493 2(8)	0.655 0(9)
O(7)	1.157 1(18)	0.541 3(8)	0.394 2(9)
O(8)	1.529 3(17)	0.502 8(8)	0.517 0(9)
O(wl)	0.099 2(24)	0.181 6(10)	0.307 4(12)
O(w2)	0.663 1(23)	0.291 7(12)	0.851 4(12)
O(w3)	0.479(3)	0.182 9(9)	0.717 7(10)
N(1)	0.773 7(23)	0.879 1(9)	0.391 8(12)
N(2)	0.913 6(22)	0.955 8(9)	0.566 7(10)
N(3)	0.550 3(21)	1.009 6(8)	0.447 3(10)
N(4)	0.870 0(22)	1.098 1(9)	0.451 1(12)
N(5)	1.067 7(22)	0.393 1(9)	0.654 2(11)
N(6)	1.199 1(22)	0.467 0(9)	0.832 3(11)
N(7)	0.833 8(22)	0.517 5(8)	0.712 1(11)
N(8)	1.144 4(21)	0.611 3(9)	0.720 1(11)
C(1)	0.890(3)	0.835 7(11)	0.479 1(15)
C(2)	0.870(3)	0.873 7(11)	0.579 5(18)
C(3)	0.527(3)	1.091 4(12)	0.476 0(15)
C(4)	0.671(3)	1.137 7(12)	0.426 7(17)
C(5)	0.885 4(25)	1.014 0(10)	0.223 9(12)
C(6)	1.088(3)	0.991 8(11)	0.289 6(14)
C(7)	0.559(3)	0.851 3(12)	0.367 5(16)
C(8)	0.989(3)	1.122 8(12)	0.551 9(18)
C(9)	1.188(3)	0.348 9(12)	0.741 6(16)
C(10)	1.160(3)	0.383 9(11)	0.841 8(15)
C(11)	0.807(3)	0.596 4(11)	0.750 4(14)
C(12)	0.947(3)	0.647 1(11)	0.700 7(17)
C(13)	1.174(3)	0.525 2(11)	0.488 7(13)
C(14)	1.373 3(24)	0.505 4(11)	0.557 0(14)
C(15)	0.864(3)	0.361 3(13)	0.626 3(15)
C(16)	1.263(3)	0.634 5(12)	0.824 0(17)

Table 3 Positional parameters and their e.s.d.s for compound **3**

Atom	*x*	*y*	*z*
I	−0.4886(1)	0.1796(2)	0.1690(1)
Co	−0.1966(2)	0.1535(3)	0.0004(2)
O(1)	−0.1689(8)	0.415(1)	0.0142(9)
O(2)	−0.0463(8)	0.126(1)	0.0682(8)
O(3)	−0.0331(9)	0.616(1)	0.0762(9)
O(4)	0.1045(9)	0.298(2)	0.129(1)
N(1)	−0.239(1)	0.139(2)	0.104(1)
N(2)	−0.220(1)	−0.120(2)	−0.008(1)
N(3)	−0.347(1)	0.208(2)	−0.080(1)
N(4)	−0.152(1)	0.153(2)	−0.098(1)
C(1)	−0.228(2)	−0.064(3)	0.134(1)
C(2)	−0.274(1)	−0.174(2)	0.053(1)
C(3)	−0.329(1)	0.279(3)	−0.156(1)
C(4)	−0.248(1)	0.162(3)	−0.179(2)
C(5)	−0.068(1)	0.452(2)	0.058(1)
C(6)	0.008(1)	0.280(2)	0.090(1)
C(7)	−0.183(2)	0.251(3)	0.184(1)
C(8)	−0.418(1)	0.326(3)	−0.053(1)

The ^1H NMR spectrum of pure complex **1**, which is less well resolved due to its relative insolubility in water, is shown in Fig. 8(*c*); that of pure **2** is shown in Fig. 8(*a*) and that of pure **3** in Fig. 9(*a*). Complex **1** is a racemate the cations of which are an enantiomorphic pair characterized by chiroptical symbols $\Lambda(R,S)/\Delta(S,R)$, where *R* and *S* refer to the chirality of the methylated nitrogens. This compound was an unexpected product precipitated selectively by the polymeric anions $(Pb_2Cl_5)_n$, and produced during the oxidation of Co^{2+} by PbO_2 in the presence of oxalate and meen (see ref. 11). Selective

Table 4 Bond distances (Å), angles (°) and selected hydrogen bonds for compound **1**

Pb(1)–Cl(1)	2.903(0)	Pb(2)–Cl(5)	2.860(0)	O(1)–C(5)	1.248(9)	N(3)–C(3)	1.475(12)
Pb(1)–Cl(2)	2.866(3)	Pb(2)–Cl(6)	2.737(2)	O(2)–C(6)	1.239(10)	N(4)–C(4)	1.495(12)
Pb(1)–Cl(3)	2.882(2)	Co–O(1)	1.916(6)	O(3)–C(5)	1.240(10)	N(4)–C(8)	1.457(12)
Pb(1)–Cl(4)	2.857(3)	Co–O(2)	1.900(5)	O(4)–C(6)	1.252(10)	C(1)–C(2)	1.540(13)
Pb(1)–Cl(6)	3.011(2)	Co–N(1)	1.979(7)	N(1)–C(1)	1.517(12)	C(3)–C(4)	1.505(13)
Pb(2)–Cl(2)	2.990(3)	Co–N(2)	1.898(7)	N(1)–C(7)	1.480(11)	C(5)–C(6)	1.539(11)
Pb(2)–Cl(3)	2.931(2)	Co–N(3)	1.942(7)	N(2)–C(2)	1.497(11)	O(w2)–H(w1)	0.999(10)
Pb(2)–Cl(4)	2.903(3)	Co–N(4)	1.994(7)				

Cl(1)–Pb(1)–Cl(2)	108.4(1)	Cl(3)–Pb(2)–Cl(4)	78.70(7)	O(2)–Co–N(2)	88.0(3)	C(1)–N(1)–C(7)	107.7(7)
Cl(1)–Pb(1)–Cl(3)	103.2(1)	Cl(3)–Pb(2)–Cl(5)	93.63(5)	O(2)–Co–N(3)	175.8(3)	Co–N(3)–C(3)	111.3(6)
Cl(1)–Pb(1)–Cl(4)	167.0(1)	Cl(3)–Pb(2)–Cl(6)	79.18(7)	O(2)–Co–N(4)	91.1(3)	Co–N(4)–C(4)	106.2(6)
Cl(1)–Pb(1)–Cl(6)	90.63(5)	Cl(4)–Pb(2)–Cl(5)	171.0(1)	N(1)–Co–N(2)	87.7(3)	Co–N(4)–C(8)	118.5(6)
Cl(2)–Pb(1)–Cl(3)	82.61(7)	Cl(4)–Pb(2)–Cl(6)	81.83(7)	N(1)–Co–N(3)	92.7(3)	C(4)–N(4)–C(8)	111.5(7)
Cl(2)–Pb(1)–Cl(4)	84.35(8)	Cl(5)–Pb(2)–Cl(6)	92.12(5)	N(1)–Co–N(4)	177.8(3)	N(1)–C(1)–C(2)	103.3(7)
Cl(2)–Pb(1)–Cl(6)	153.9(1)	Pb(1)–Cl(1)–Pb(1)	180.0(1)	N(2)–Co–N(3)	94.8(3)	N(2)–C(2)–C(1)	109.5(8)
Cl(3)–Pb(1)–Cl(4)	80.24(7)	Pb(1)–Cl(2)–Pb(2)	159.6(1)	N(2)–Co–N(4)	90.9(3)	N(3)–C(3)–C(4)	106.5(8)
Cl(3)–Pb(1)–C(6)	75.64(6)	Pb(1)–Cl(3)–Pb(2)	84.88(6)	N(3)–Co–N(4)	85.7(3)	N(4)–C(4)–C(3)	107.5(8)
Cl(4)–Pb(1)–Cl(6)	78.02(7)	Pb(1)–Cl(4)–Pb(2)	85.84(7)	O(1)–Co–N(3)	93.1(3)	O(1)–C(5)–O(3)	125.3(8)
Cl(2)–Pb(2)–Cl(3)	157.5(1)	Pb(1)–Cl(6)–Pb(2)	85.92(6)	O(1)–Co–N(4)	92.1(3)	O(1)–C(5)–C(6)	112.2(7)
Cl(2)–Pb(2)–Cl(4)	80.05(7)	O(1)–Co–O(2)	84.2(2)	O(2)–Co–N(1)	90.5(3)	O(3)–C(5)–C(6)	122.5(8)
Cl(2)–Pb(2)–Cl(5)	106.8(1)	O(1)–Co–N(1)	89.5(3)	Co–N(1)–C(1)	109.5(6)	O(2)–C(6)–C(5)	116.2(8)
Cl(2)–Pb(2)–Cl(6)	90.66(7)	O(1)–Co–N(2)	171.7(3)	Co–N(1)–C(7)	121.0(6)	O(4)–C(6)–C(5)	120.0(8)

Selected hydrogen bonds

Cl(2)···H(6)	2.44	O(3)···H(8)	2.39	N(2^{I})–H(6)···Cl(2)	172.6	N(3^{II})–H(8)···O(3)	147.7
Cl(3)···H(7)	2.87	O(4)···H(7)	2.08	N(3^{I})–H(7)···Cl(3)	106.8	N(2^{II})–H(7)···O(4)	154.2
Cl(3)···H(14)	2.71	O(4)···H(8)	2.33	N(4^{I})–H(14)···Cl(3)	144.6	N(3^{II})–H(8)···O(4)	136.5
Cl(6)···H(9)	2.34	O(wl)···H(1)	2.10	N(3)–H(9)···Cl(6)	153.1	N(1)–H(1)···O(wl)	154.4
O(2)···H(1)	2.43			N(1)–H(1)···O(2)	100.0		

Symmetry relations: I $-1 + x, y, z$; II $-\frac{1}{2} + x, \frac{1}{2} - y, -\frac{1}{2} + z$.

Table 5 Bond distances (Å), angles (°) and selected hydrogen bonds for compound **2**

Co(1)–O(1)	1.932(11)	Co(2)–N(8)	1.972(16)	O(w2)–H(w3)	0.715(15)	N(6)–C(10)	1.48(3)
Co(1)–O(2)	1.922(11)	O(1)–C(5)	1.284(20)	O(w3)–H(w4)	0.671(14)	N(7)–C(11)	1.486(24)
Co(1)–N(1)	1.981(15)	O(2)–C(6)	1.287(21)	O(w3)–H(w5)	1.039(17)	N(8)–C(12)	1.46(3)
Co(1)–N(2)	1.914(14)	O(3)–C(5)	1.224(19)	N(1)–C(1)	1.465(25)	N(8)–C(16)	1.49(3)
Co(1)–N(3)	1.922(14)	O(4)–C(6)	1.223(21)	N(1)–C(7)	1.51(3)	C(1)–C(2)	1.47(3)
Co(1)–N(4)	1.956(15)	O(5)–C(13)	1.283(21)	N(2)–C(2)	1.479(25)	C(3)–C(4)	1.48(3)
Co(2)–O(5)	1.945(12)	O(6)–C(14)	1.277(21)	N(3)–C(3)	1.490(24)	C(5)–C(6)	1.532(23)
Co(2)–O(6)	1.919(13)	O(7)–C(13)	1.228(20)	N(4)–C(4)	1.50(3)	C(9)–C(10)	1.46(3)
Co(2)–N(5)	1.950(15)	O(8)–C(14)	1.247(20)	N(4)–C(8)	1.47(3)	C(11)–C(12)	1.51(3)
Co(2)–N(6)	1.931(15)	O(w1)–H(w1)	1.047(18)	N(5)–C(9)	1.48(3)	C(13)–C(14)	1.520(24)
Co(2)–N(7)	1.916(14)	O(w1)–H(w2)	0.827(15)	N(5)–C(15)	1.47(3)		

O(1)–Co(1)–O(2)	84.4(5)	O(6)–Co(2)–N(8)	90.7(6)	C(1)–N(1)–C(7)	111.5(15)	O(2)–C(6)–O(4)	124.8(16)
O(1)–Co(1)–N(1)	89.8(6)	N(5)–Co(2)–N(6)	85.8(7)	Co(1)–N(2)–C(2)	111.0(12)	O(2)–C(6)–C(5)	114.5(14)
O(1)–Co(1)–N(2)	173.9(6)	N(5)–Co(2)–N(7)	95.3(6)	Co(1)–N(3)–C(3)	111.0(11)	O(4)–C(6)–C(5)	120.6(16)
O(1)–Co(1)–N(3)	89.3(5)	N(5)–Co(2)–N(8)	177.9(6)	Co(1)–N(4)–C(4)	106.8(12)	N(5)–C(9)–C(10)	108.0(16)
O(1)–Co(1)–N(4)	88.2(6)	N(6)–Co(2)–N(7)	94.5(6)	Co(1)–N(1)–C(1)	107.1(12)	N(6)–C(10)–C(9)	106.7(16)
O(2)–Co(1)–N(1)	88.3(6)	N(6)–Co(2)–N(8)	95.8(7)	Co(1)–N(1)–C(7)	117.8(12)	N(7)–C(11)–C(12)	106.5(15)
O(2)–Co(1)–N(2)	91.5(5)	N(7)–Co(2)–N(8)	86.0(6)	Co(1)–N(4)–C(8)	119.5(12)	N(8)–C(12)–C(11)	107.3(16)
O(2)–Co(1)–N(3)	172.7(6)	Co(1)–O(1)–C(5)	113.6(10)	C(4)–N(4)–C(8)	113.0(15)	O(5)–C(13)–O(7)	123.3(16)
O(2)–Co(2)–N(7)	90.4(6)	Co(1)–O(2)–C(6)	113.5(10)	Co(2)–N(5)–C(9)	107.4(11)	O(5)–C(13)–C(14)	113.5(14)
O(5)–Co(2)–N(8)	88.6(6)	Co(2)–O(5)–C(13)	113.2(11)	Co(2)–N(5)–C(15)	119.9(13)	O(7)–C(13)–C(14)	123.2(16)
O(6)–Co(2)–N(5)	87.8(6)	Co(2)–O(6)–C(14)	112.8(11)	O(1)–C(5)–O(3)	123.5(15)	O(6)–C(14)–O(8)	123.8(15)
O(6)–Co(2)–N(6)	91.0(6)	H(w1)–O(w1)–H(w2)	96.6(15)	O(1)–C(5)–C(6)	113.9(13)	O(6)–C(14)–C(13)	116.1(14)
O(6)–Co(2)–N(7)	173.9(6)	H(w4)–O(w3)–H(w5)	112.8(18)	O(3)–C(5)–C(6)	122.6(15)	O(8)–C(14)–C(13)	120.0(15)

Selected hydrogen bonds

Br(1)···H(21)	2.52	O(3)···H(8)	2.08	N(5^{I})–H(21)···Br(1)	143.0	N(3^{VIII})–H(8)···O(3)	146.2
Br(2)···H(w2)	2.51	O(4)···H(6)	2.04	O(wl^{II})–H(w2)···Br(2)	155.0	N(2^{VIII})–H(6)···O(4)	157.4
Br(2)···H(w3)	2.56	O(4)···H(9)	2.08	O(w2^{III})–H(w3)···Br(2)	166.3	N(3^{II})–H(9)···O(4)	170.9
Br(2)···H(34)	2.46	O(7)···H(27)	2.15	N(8^{IV})–H(34)···Br(2)	150.9	N(6^{IV})–H(27)···O(7)	162.1
O(wl)···H(14)	2.07	O(7)···H(28)	2.12	N(4^{V})–H(14)···O(wl)	158.1	N(7^{IX})–H(28)···O(7)	148.5
O(w2)···H(w5)	1.74	O(8)···H(26)	1.99	O(w3)–H(w5)···O(w2)	155.3	N(6^{X})–H(26)···O(8)	148.4
O(w3)···H(1)	2.11	O(8)···H(29)	2.03	N(1^{VI})–H(1)···O(w3)	159.7	N(7^{II})–H(29)···O(8)	172.2
O(3)···H(7)	2.10			N(2^{VII})–H(7)···O(3)	172.9		

Symmetry relations: I $x - 1, y, z$; II $x + 1, y, z$; III $x, y, z - 1$; IV $x - \frac{1}{2}, 1 - y, z - \frac{1}{2}$; V $x - 1, y - 1, z$; VI $x - \frac{1}{2}, 1 - y, z + \frac{1}{2}$; VII $x - \frac{1}{2}, 2 - y, z - \frac{1}{2}$; VIII $x + \frac{1}{2}, 2 - y, z - \frac{1}{2}$; IX $x + \frac{1}{2}, 1 - y, 1 - z$; X $x + \frac{1}{2}, 1 - y, z - \frac{1}{2}$.

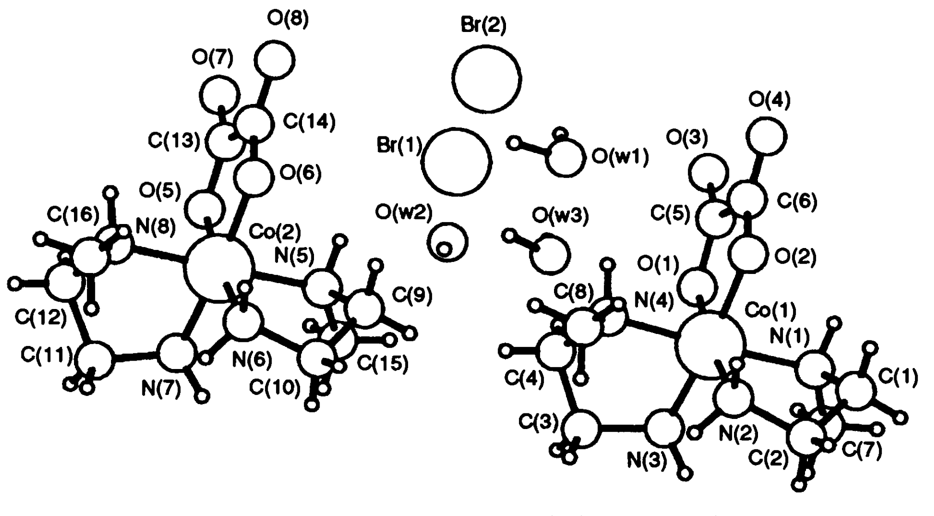

Fig. 2 Contents of the asymmetric unit present in compound **2** displaying the numbering system used

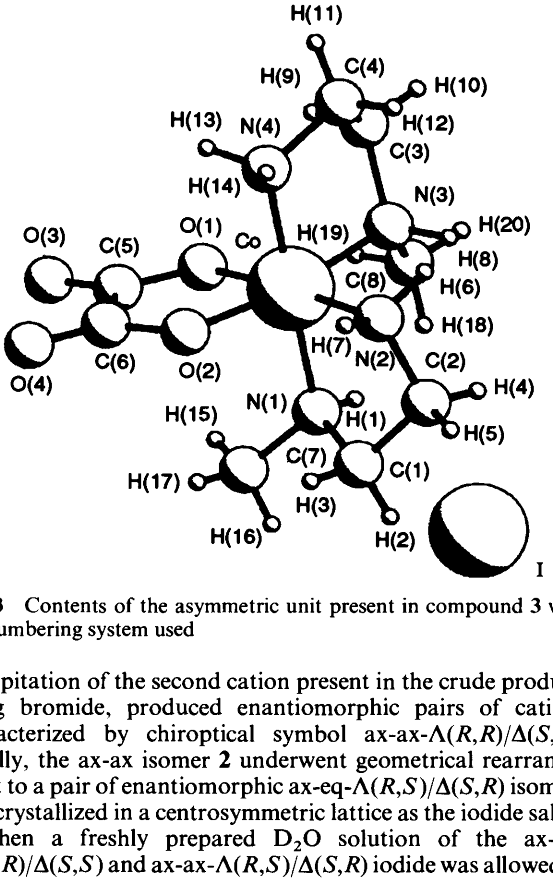

Fig. 3 Contents of the asymmetric unit present in compound **3** with the numbering system used

precipitation of the second cation present in the crude product, using bromide, produced enantiomorphic pairs of cations characterized by chiroptical symbol ax-ax-$\Lambda(R,R)/\Delta(S,S)$. Finally, the ax-ax isomer **2** underwent geometrical rearrangement to a pair of enantiomorphic ax-eq-$\Lambda(R,S)/\Delta(S,R)$ isomers and crystallized in a centrosymmetric lattice as the iodide salt **3**.

When a freshly prepared D_2O solution of the ax-ax-$\Lambda(R,R)/\Delta(S,S)$ and ax-ax-$\Lambda(R,S)/\Delta(S,R)$ iodide was allowed to stand for 7 d at 20 °C a new spectrum was observed. As shown in Fig. 9(*b*) and 9(*c*) the peak at δ 2.146 disappears while another two at δ 2.137 and 1.838 ($\Delta = 0.299$ ppm), appear. The peaks for the methyl groups of the ax-ax-$\Lambda(R,S)/\Delta(S,R)$ isomers remained unchanged. Therefore, it is the ax-ax-$\Lambda(R,R)/\Delta(S,S)$ isomers which are unstable and underwent 100% rearrangement. The new pair created is described as the ax-eq-$\Lambda(R,S)/\Delta(S,R)$ enantiomers, which are precipitated as the iodide salts. It is strange that the rearrangement produces two isomers, the ax-eq- and ax-ax-$\Lambda(R,S)/\Delta(S,R)$, since the ratio of the two isomers changed from 74:36 to 68:32. The ax-eq-$\Lambda(R,S)/\Delta(S,R)$ isomer is the major rearranged product. In order to explore the role of the KI in the rearrangement another NMR spectrum was taken for $[Co(meen)_2(C_2O_4)]X$ ($X = Br$ or Pb_2Cl_5) after being kept in D_2O at 20 °C for 7 d. As shown in Fig. 8(*c*) and 8(*d*), for $X = Pb_2Cl_5$, the chemical shifts of the

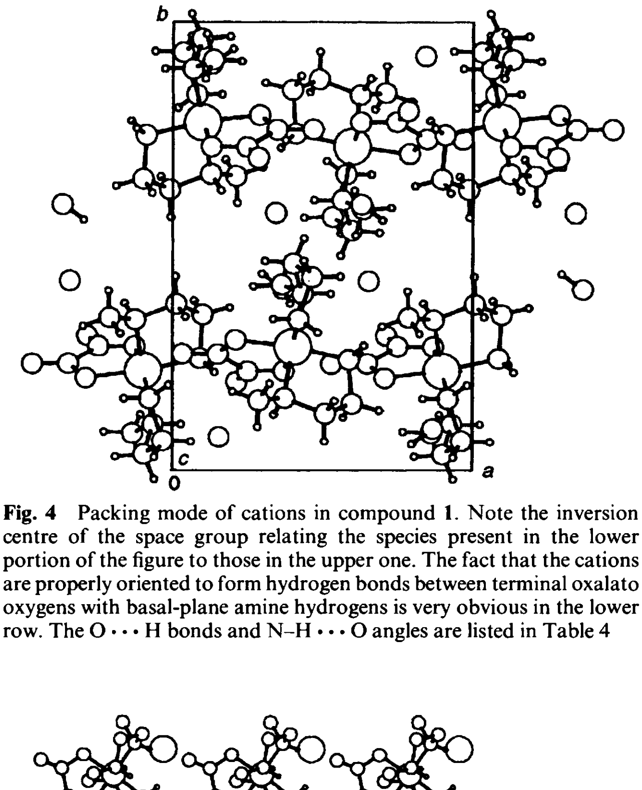

Fig. 4 Packing mode of cations in compound **1**. Note the inversion centre of the space group relating the species present in the lower portion of the figure to those in the upper one. The fact that the cations are properly oriented to form hydrogen bonds between terminal oxalato oxygens with basal-plane amine hydrogens is very obvious in the lower row. The O $\cdots$ H bonds and N–H $\cdots$ O angles are listed in Table 4

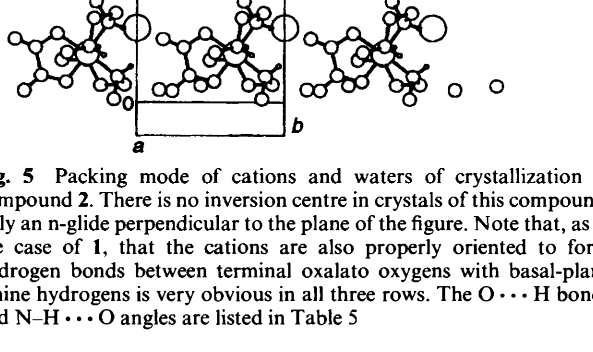

Fig. 5 Packing mode of cations and waters of crystallization in compound **2**. There is no inversion centre in crystals of this compound, only an n-glide perpendicular to the plane of the figure. Note that, as in the case of **1**, that the cations are also properly oriented to form hydrogen bonds between terminal oxalato oxygens with basal-plane amine hydrogens is very obvious in all three rows. The O $\cdots$ H bonds and N–H $\cdots$ O angles are listed in Table 5

Table 6 Bond distances (Å), angles (°) and selected hydrogen bonds for compound **3**

Co–O(1)	1.906(4)	N(1)–C(1)	1.531(8)
Co–O(2)	1.896(4)	N(1)–C(7)	1.512(9)
Co–N(1)	1.990(7)	N(2)–C(2)	1.460(9)
Co–N(2)	1.982(5)	N(3)–C(3)	1.458(9)
Co–N(3)	1.990(5)	N(3)–C(8)	1.417(8)
Co–N(4)	1.922(7)	N(4)–C(4)	1.507(8)
O(1)–C(5)	1.286(7)	C(1)–C(2)	1.513(10)
O(2)–C(6)	1.290(6)	C(3)–C(4)	1.482(10)
O(3)–C(5)	1.256(7)	C(5)–C(6)	1.551(8)
O(4)–C(6)	1.203(7)		
O(1)–Co–O(2)	85.2(2)	Co–N(1)–C(7)	123.5(4)
O(1)–Co–N(1)	92.2(2)	C(1)–N(1)–C(7)	104.5(6)
O(1)–Co–N(2)	177.2(2)	Co–N(2)–C(2)	107.6(4)
O(1)–Co–N(3)	89.4(2)	Co–N(3)–C(3)	105.7(4)
O(1)–Co–N(4)	90.6(2)	Co–N(3)–C(8)	118.7(5)
O(2)–Co–N(1)	89.3(2)	C(3)–N(3)–C(8)	111.6(6)
O(2)–Co–N(2)	92.3(2)	Co–N(4)–C(4)	112.7(4)
O(2)–Co–N(3)	171.9(2)	N(1)–C(1)–C(2)	103.7(6)
O(2)–Co–N(4)	89.0(2)	N(2)–C(2)–C(1)	110.9(6)
N(1)–Co–N(2)	86.4(2)	N(3)–C(3)–C(4)	110.6(7)
N(1)–Co–N(3)	96.9(3)	N(4)–C(4)–C(3)	103.2(7)
N(1)–Co–N(4)	176.7(2)	O(1)–C(5)–O(3)	123.0(6)
N(2)–Co–N(3)	93.2(2)	O(1)–C(5)–C(6)	115.3(5)
N(2)–Co–N(4)	90.8(2)	O(3)–C(5)–C(6)	121.7(5)
N(3)–Co–N(4)	85.0(3)	O(2)–C(6)–O(4)	127.0(5)
Co–O(1)–C(5)	112.7(4)	O(2)–C(6)–C(5)	111.5(5)
Co–O(2)–C(6)	115.2(4)	O(4)–C(6)–C(5)	121.5(5)
Co–N(1)–C(1)	107.8(5)		
Selected hydrogen bonds			
I · · · H(8)	2.61	N(3^{I})–H(8) · · · I	157.7
O(1) · · · H(13)	2.51	N(4^{II})–H(13) · · · O(1)	92.2
O(2) · · · H(14)	2.26	N(4^{III})–H(14) · · · O(2)	78.1
O(3) · · · H(7)	2.15	N(2^{IV})H(7) · · · O(3)	150.4
O(3) · · · H(13)	1.92	N(4^{V})–H(13) · · · O(3)	155.3
O(4) · · · H(14)	2.49	N(4^{VI})–H(14) · · · O(4)	151.0

Symmetry relations: I $-x-1, -y, -z$; II $x-1, y, z-1$; III $-x, -y-1, -z$; IV $x, y+1, z$; V $-x, 1-y, z$; VI $-x, -y, -z$.

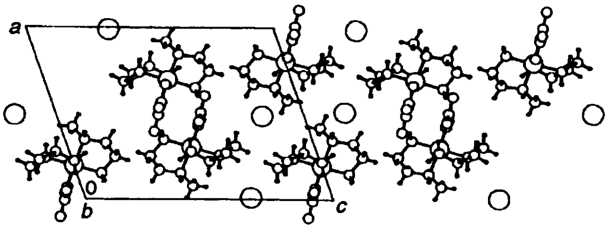

Fig. 6 Packing mode of cations and waters of crystallization in compound 3. Note the inversion centre of the space group relating the species present in the lower portion of the figure to those in the upper one. The fact that the cations are improperly oriented to form hydrogen bonds between terminal oxalato oxygens with basal-plane amine hydrogens is very obvious since the oxalate ligands of the lower and upper rows point into each other as well as to axial amine hydrogens. The O · · · H bonds and N–H · · · O angles are listed in Table 6

methyl groups remain the same, except that the peaks change from a doublet to a singlet. However, with X = Br, two new peaks were observed with Δ = 0.331 ppm, which belong to the ax-ax-Λ(*R*,*S*)/Δ(*S*,*R*) isomer. The ratio of the two isomers is 83:17. In other words, only 17% of the (*R*,*R*) isomer undergoes rearrangement within 7 d, Fig. 8(*c*). Thus the ax-eq-Λ-(*R*,*S*)/Δ(*S*,*R*) isomer is produced exclusively in the presence of KI, while with NH_4Br ax-ax-Λ(*R*,*S*)/Δ(*S*,*R*) is produced. The latter isomer is the most stable one, no rearrangement at room temperature being observed in the presence of $Pb_2Cl_5^-$, Cl^- or I^-. Thus, the ax-ax-Λ(*R*,*R*)/Δ(*S*,*S*) enantiomeric pair are probably kinetic products while the ax-ax- and ax-eq-Λ(*R*,*S*)/Δ(*S*,*R*) are thermodynamic products.

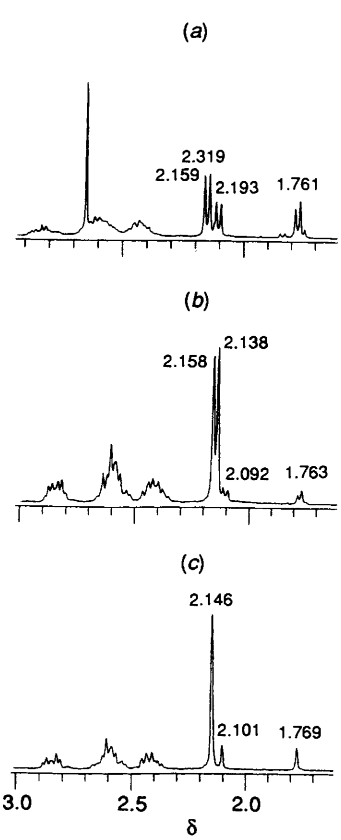

Fig. 7 Proton NMR (D_2O) spectra of $[Co(meen)_2(C_2O_4)]X{\cdot}nH_2O$ where X = Cl (*a*), Br (*b*) or I (*c*)

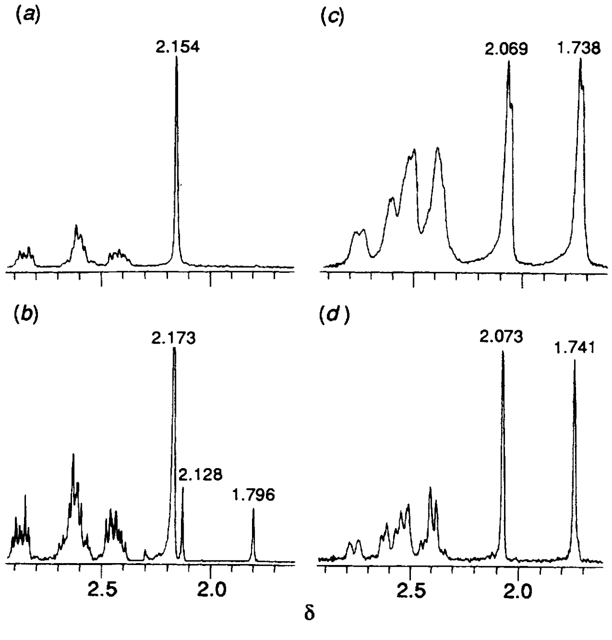

Fig. 8 Proton NMR (D_2O) spectra of $[Co(meen)_2(C_2O_4)]X{\cdot}nH_2O$ where X = Br (*a* and *b*) or Pb_2Cl_5 (*c* and *d*). Spectra (*b*) and (*d*) were recorded after 7 d at 20 °C

Discussion

In the past we found that compounds of the series $[Co(en)_2(C_2O_4)]X{\cdot}nH_2O$ (X = Cl, *n* = 4; Br, 1; I, 0)[12] crystallize as conglomerates if two conditions are met: (*a*) the formation of spiral strings of cations held together by strong O · · · H_2N hydrogen bonds in which a terminal oxalato oxygen binds, in a bidentate fashion, a pair of basal-plane hydrogens of an

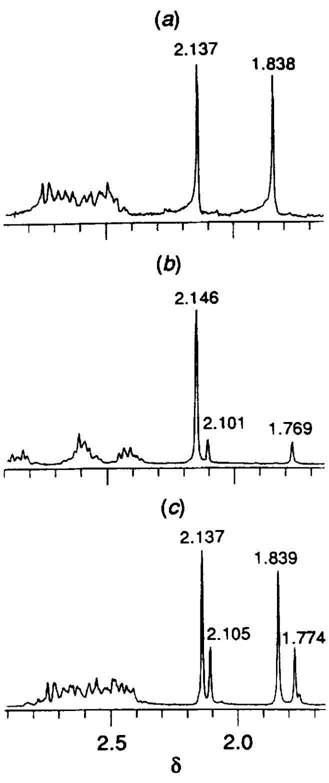

Fig. 9 Proton NMR (D_2O) spectra of [Co(meen)$_2$(C_2O_4)]I. Isomers: (*a*) ax-eq (*R,S*)/(*S,R*); (*b*) ax-ax-(*R,R*)/(*S,S*) + -(*R,S*)/(*S,R*); (*c*) ax-ax- + ax-eq-(*R,S*)/(*S,R*). The differences Δ in chemical shift between the two methyl groups of the same ligand are 0.299 (*a*), 0.331 (*b*) and 0.331 (Δ_1), 0.299 ppm (Δ_2) (*c*)

adjacent cation, while the second terminal oxygen binds a third hydrogen, giving rise to a three-point chiral recognition pattern; (*b*) the spirals are then hydrogen bonded to one another by the counter anions (and waters of crystallization, if any); and, if the more advantageous hydrogen-bonding scheme is obtained by linking strings of the same chirality. Other types of crystals (racemates, kryptoracemates, *etc.*) are obtained otherwise.

Here, we remind the reader that in a previous report by Marusak *et al.*[5] crystals of $\Delta(\lambda\delta)$-[Co{*trans*-(dmen)$_2$}(C_2O_4)]I **4** and of $\Delta(\delta\delta)$-[Co(*R,S*-*R,S*-dmen)$_2$(C_2O_4)]I·$2H_2O$ **5** were said to crystallize, respectively, in space groups *Pbca* and $P2_1$. Thus, the former is a racemate while the latter is a conglomerate in which both axial nitrogens have chirality *R* and both equatorial ones *S*, results which can be understood on the basis of our cited experiences with the amine oxalates of cobalt described in the above paragraph.[12] Briefly, in [Co(en)$_2$(C_2O_4)]X·*n*H_2O (X = Cl, *n* = 4; Br, 1; I, 0)[12] as well as in $\Delta(\delta\delta)$-[Co(*R,S*-*R,S*-dmen)$_2$(C_2O_4)]I·$2H_2O$[5] spiral strings are formed (the previous authors[5] did not provide packing diagrams so we generated one, each, in order to demonstrate the validity of our claims; see Figs. 10 and 11 for the packing in **4** and **5**, respectively). In the conglomerate **5** spiral strings are clearly seen in Fig. 10, where terminal oxalato oxygens are shown to form the expected three-point attachments to the basal plane NH hydrogens of adjacent cations.

In the case of the racemate,[5] spiral strings of hydrogen-bonded cations are, theoretically, possible since the basal plane contains two NH_2 moieties; however, the axial amino nitrogens are dimethylated and, thus, the theoretical spiral strings cannot be stitched to one another, since it is these hydrogens which are needed to do so. Note instead (Fig. 11 and its caption) that the oxalate ligand of a given cation points at a single NH_2 of another one in an adjacent row. This is most clearly seen in the left-most column (along the *b* axis) of Fig. 11.

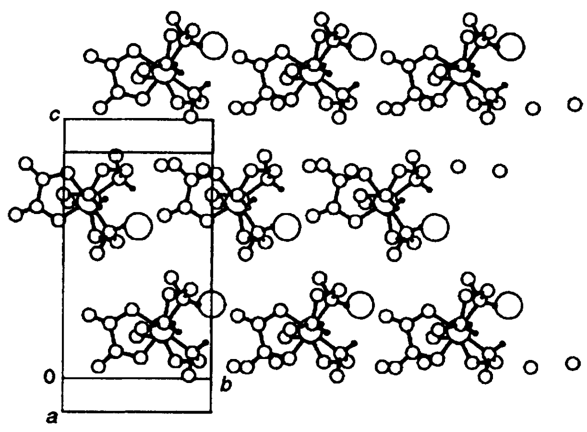

Fig. 10 Crystal packing in complex **4**. Note the spiral strings running along the *b* axis in which, through a three-point hydrogen-bonded attachment, most clearly shown in the lower left pair of cations, the two terminal oxygens of oxalate bond to two basal-plane, amine hydrogens of an adjacent one. This pattern of hydrogen bonding is infinitely repeated and the outcome is an infinite spiral string as most readily seen in the middle row [H(2)···O(3) 2.52, H(2)···O(4) 2.25 and H(3)···O(4) 2.24 Å]. Spiral strings are then stitched together by the agency of hydrogen bonds with the axial amines. This is also true of the halides of composition [Co(en)$_2$(C_2O_4)]X·*n*H_2O (X = Cl, *n* = 4; Br, 1; I, 0)[12] in spite of the differences in waters of hydration. For details the reader is referred to ref. 2. The results of Marusak *et al.*[5] for the conglomerate are, thus, in agreement with our observations

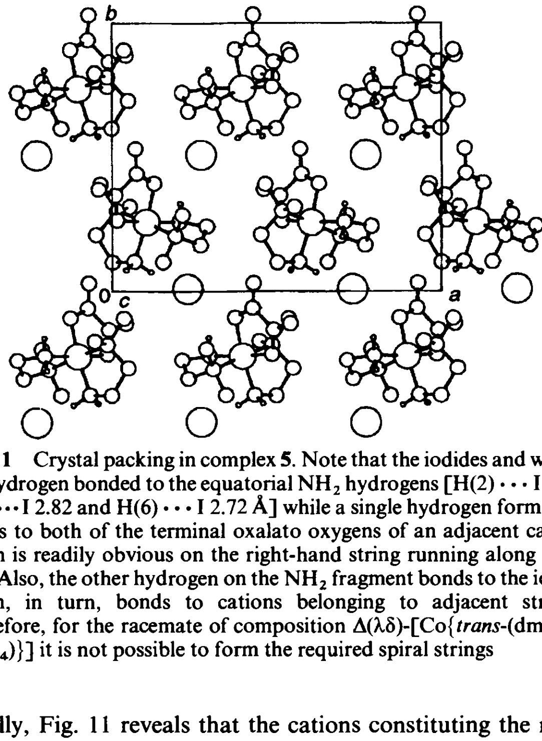

Fig. 11 Crystal packing in complex **5**. Note that the iodides and waters are hydrogen bonded to the equatorial NH_2 hydrogens [H(2)···I 2.92, H(5)···I 2.82 and H(6)···I 2.72 Å] while a single hydrogen forms two bonds to both of the terminal oxalato oxygens of an adjacent cation, which is readily obvious on the right-hand string running along the *b* axis. Also, the other hydrogen on the NH_2 fragment bonds to the iodide which, in turn, bonds to cations belonging to adjacent strings. Therefore, for the racemate of composition $\Delta(\lambda\delta)$-[Co{*trans*-(dmen)$_2$(C_2O_4)}] it is not possible to form the required spiral strings

Finally, Fig. 11 reveals that the cations constituting the rows running along the *a* axis alternate in chirality. In all three strings shown the sequence of chiral symbols of these cations is $(..\Delta....\Lambda....\Delta....\Lambda..)_n$ while all cations of the strings running along the *b* axis are exclusively Λ or Δ.

We searched the literature for published data on Co(meen)$_2$ derivatives but found no structural studies of these species. Searle and Keene[13] stated that complexes of meen which have been studied include tris complexes [Co(meen)$_3$]Cl_3 and [Ni(meen)$_3$]Br_2.[14] The effect of substitution at N on the spectroscopic properties of the nickel complexes was examined by Pavkovic and Meek[15] but the isomers of these tris(meen) complexes have never been separated or characterized. Particular isomers have, however, been isolated for several bis and mono complexes, $[Co(meen)_2X_2]^+$ [16-20] $[Co(meen)_2(en)]^{3+}$ [21], $[Co(meen)(NH_3)_4]^{3+}$ (refs. 15, 22, 23) and $[Co(meen)(CN)]^{2+}$ [23] with their configurations being assigned from crystal structure [20] and electronic, circular dichroism and NMR spectral comparisons [19,21] and by conformational analysis considerations.[19,23] Of primary interest in studies of these complexes has been the effect of *N*-methyl substitution on various properties, including optical rotatory properties,[19-21,24,25] kinetics of proton exchanges and racemization,[18,22] conformational analysis by NMR spectroscopy [23] and reactivity and stabilities of some isomers.[19] The stereochemistry present in these meen complexes is complicated since $[Co(meen)(C_2O_4)]^+$ cations can exist in three possible geometries arising from the relative positions of the NH_2 and NMe moieties of the two meen ligands. Each geometrical isomer can exist in several possible diastereoisomeric forms, giving in all ten distinct forms for each absolute configuration (Λ or Δ) at Co. Those arising from the Λ complex configuration are shown in Scheme 1, along with their designations.

Each of these ten diastereoisomeric forms has four conformational combinations for the Co(meen) rings, δδ, λλ, λδ and δλ. Models show that the dominant non-bonded interactions should be those of the *N*-methyl groups with neighbouring rings (Me ··· Me, Me ··· ring, Me ··· NH_2 or Me ··· NH) and that these should significantly influence the relative stabilities of the isomers. Interring H ··· H interactions between NH_2 and CH_2 groups of the type causing *lel* conformations to be preferred in $[Co(en)_2]^{3+}$ [26] may be of relatively less importance in these $[Co(meen)_2]$ systems.

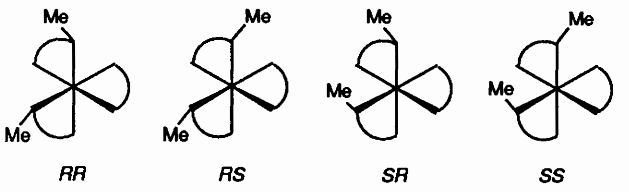

Λ *cis*-Me, *cis*-NH_2(ax-eq)

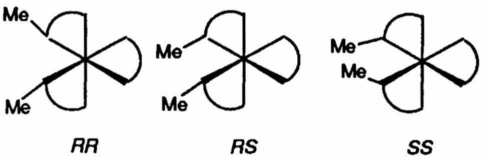

Λ *cis*-Me,*trans*-NH_2(eq-eq)

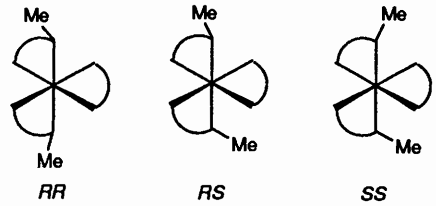

Λ *trans*-Me, *cis*-NH_2(ax-ax)

Scheme 1 Possible geometric isomers and diastereoisomers for $[Co(meen)_2(C_2O_4)]^+$

Stereochemical Character of the Cations present in Complexes **1**–**3**.—The structure of the $Pb_2Cl_5^-$ anions present in the lattice of complex **1** has been published before and will not be repeated here except to mention that it is an infinite, polymeric, entity which resembles a clathrate. The tubular holes running approximately along [011] contain the cations and waters of crystallization. However, in order to show the interaction between the cations and waters, Fig. 4 is presented.

When the structure [8] of the cations present in crystals of complex **1** was established, the NMR spectrum obtained for D_2O solutions of pure single crystals began to clarify the nature of the complicated spectrum obtained for the crude reaction product. Briefly, Fig. 4 shows that the cations are present in the lattice in racemic pairs describable as *meso*-Λ(δλ)-[Co{*trans*-(*R*,*S*)(meen)$_2$}(C_2O_4)][Pb_2Cl_5]·$2H_2O$ and *meso*-Δ(λδ)-[Co{*trans*-(*S*,*R*)(meen)$_2$}(C_2O_4)][Pb_2Cl_5]·$2H_2O$. A model of the cation reveals that the NH(Me) fragments are not equivalent. One is located above the non-bonded pair of electrons of an oxalate oxygen, the other in between an oxalate oxygen and an ethylenediamine NH_2, with $\Delta = 0.331$ ppm, where Δ is the chemical shift difference between the two methyl groups. When the NMR spectrum obtained from single crystals of **1** is compared with that of the crude product of the reaction it is clear that the synthetic procedure produces two geometrical isomers, that described above and another in which the methyl protons of the amines are equivalent. Again, a model shows that the methyl groups of the diastereoisomeric cation Λ(λλ)-[{[Co{*trans*-(*R*,*R*)(meen)$_2$}(C_2O_4)]Br}$_2$]·$3H_2O$ **2** are located in the same environments, *e.g.* between an oxalate oxygen and an ethylenediamine NH_2. The same is, of course, true of its enantiomer; thus the enantiomeric pair of cations Λ(λλ)-[{[Co{*trans*-(*R*,*R*)(meen)$_2$}(C_2O_4)]Br}$_2$]·$3H_2O$ and Δ(δδ)-[{[Co{*trans*-(*S*,*S*)(meen)$_2$}(C_2O_4)]Br}$_2$]·$3H_2O$ are responsible for the methyl doublet of the ^1H NMR spectrum described above [see Fig. 7(*a*)].

Cations in complex **1** pack in strings (see Fig. 4) which run through the length of the tunnels of the $(Pb_2Cl_5^-)_n$ clathrate cage; thus, the strings are isolated from one another. Fig. 4 is a *c* projection selected because it shows the nature of the strings which are held together by three hydrogen bonds between the terminal oxygens [O(3) and O(4)] of oxalate and hydrogens [H(7) and H(8)] on adjacent, equatorial, amine hydrogens [O(3) ··· H(8) 2.393, O(4) ··· H(7) 2.084 and O(4) ··· H(8) 2.327 Å] as was expected for such species. However, in **2**, for the first and only time in our extensive studies of these amine oxalato systems, the cations within a string are heterochiral. The two cations flanking a central one in a given string are of the same chirality, but of opposite chirality to that sandwiched between them. In the middle string of Fig. 5 the pattern is $(..\Delta....\Lambda....\Delta....\Lambda..)_n$. Thus, the strings are an internally compensated chiral system and adjacent strings are related by the inversion centre of the space group, as is obvious in Fig. 5.

It is of more than passing interest that the bromide anion has a marked preference for the Λ(λλ)-[Co{*trans*-(*R*,*R*)(meen)$_2$}(C_2O_4)]$^+$ cation and its enantiomorph since it only differs from that isolated with the $Pb_2Cl_5^-$ anion in the chirality at one of the axial amines and the helical chirality of one of the en rings. Thus, we are given an opportunity of comparing their crystallization behaviour, even when the comparison is imperfect (we have proven in several cases that changing counter ions for a given chiral cobalt amine frequently results in a change in crystallization pathway; see refs. 4, 12, 27 and refs. therein). Thus, the comparison may not be appropriate until the crystallization mode of the cation present in complex **1** in the form of the bromide is determined.

As was the case with bromide, iodide also displays a marked preference for the precipitation of the Λ(λλ)-[Co{*trans*-(*R*,*R*)(meen)$_2$}(C_2O_4)]$^+$ cation, as is clear from the NMR spectrum of the freshly precipitated material [see Fig. 7(c)]; however, upon long standing in water and exposure to fluorescent light, the cation rearranges to that present in **3**, *e.g.* the Λ-(λλ)-[Co{*trans*-(*R*,*R*)(meen)$_2$}(C_2O_4)]$^+$ cations rearrange to the enantiomorphic pair *meso*-Δ(λδ)-[Co{*cis*-(*R*,*S*)(meen)$_2$}(C_2O_4)]I observed in **3**. To some extent this was of no surprise since we have previously shown that water solutions of *cis*-$[Co(en)_2(NO_2)_2]I$ [12] and $[Co(en)_2(C_2O_4)]I$ [4,28] are capable of undergoing photochemically catalysed molecular rearrangements. In the case of the oxalate, a major product is [{Co-

$(en)_3(C_2O_4)\}_2]\cdot 3H_2O$, the structure of which was determined from both the photochemical rearrangement product and from material obtained by a rational synthesis. Interestingly, we have also demonstrated that trace amounts of I_3^-, present in most old bottles of KI, catalyse molecular rearrangements in cobalt cations. For example, we demonstrated[29] that rearrangement from *cis*-β- to *cis*-α-$[Co(trien)(NO_2)_2]^+$ (trien = triethylenetetramine occurs when a water solution of *cis*-β-$[Co(trien)(NO_2)_2]Cl$ is treated with an excess of solid KI taken from an old bottle. Upon recrystallization (twice) the freshly precipitated KI produced the desired *cis*-β-$[Co(trien)(NO_2)_2]I$, the crystal structure of which we had already reported.[29]

Relative Stability of Diastereoisomers.—We noted above that the rearrangement leading to the isolation of complex **3** converts an ax-ax into an ax-eq $(MeHN)_2$ geometrical isomer, not produced during the initial synthesis described above. Thus, since it is known that the *cis*-α-trien complex is thermodynamically more stable than the *cis*-β isomer, and we noted the catalytic conversion by I_3^- of the latter into the former, it is tempting to suggest that **3** is thermodynamically more stable than **2** and its formation is triggered, as in the *cis*-β–*cis*-α pair, by I_3^-, since the isomerization takes place only in iodide solutions.

Similar arguments suggest that the cation present in complex **2** is less stable than that observed in **1** since NH_4Br solutions of the former, allowed to stand under fluorescent light, give rise to a rearrangement of the ax-ax-$\Lambda(R,R)/\Delta(S,S)$ pair present in the former to the ax-ax-$\Lambda(S,R)/\Delta(R,S)$ cation present in the latter. From the standpoint of entropy, such a rearrangement makes eminently good sense. Thus, these stereochemical changes may be entropy driven.

Crystallization Pathway followed by the Three Compounds Isolated.—The fact that all three isomers crystallize as racemates is interesting in view of the fact that two of them are axial–axial geometrical isomers and the third is an axial–equatorial one. In the former case the stereochemistry at the basal plane of these cations allows for the formation of (terminal C_2O_4 O $\cdots$ H–N) hydrogen-bonded, helical strings of the type observed with $[Co(en)_2(C_2O_4)]X\cdot nH_2O$ (X = Cl, n = 4; Br, 1; I, 0) all three of which are conglomerates. However, the *N*,*N*′-dimethylethylenediamine derivative **5** studied by Marusak *et al.*[5] has an absolute configuration $\Delta(\delta\delta)$ or $\Lambda(\lambda\lambda)$ whereas **1** is $\Delta(\lambda\delta)$ or its enantiomorph. Therefore, it appears that the axial and equatorial HNMe hydrogens in the cation studied by Marusak *et al.*[5] are properly oriented to form hydrogen-bonded strings of homochiral anions which are linked to adjacent homochiral strings. However, in **1** the strings of cations running along the *a* and *b* axes (Fig. 4) contain cations which alternate in chirality in both directions, *e.g.* the two-dimensional layer shown consists of strings that are internally compensated mesomers in both directions, exactly as in the case of the racemate **4**, see above.[5]

The bromide complex **2** contains two independent molecules in the asymmetric unit, both of which are shown in Fig. 2 as being $\Lambda(\lambda\lambda)$; however, the crystals, having a glide plane, must contain an equal number of $\Delta(\delta\delta)$ cations. Consequently, these cations have the same chiroptical symbol as those observed by Marusak *et al.*[5] for axial nitrogens of their *N*,*N*′-dimethyl iodide. Thus it is reasonable to expect that they could crystallize as a conglomerate, were it not for an additional observation; namely, that in **2** the full chiral symbol of the cation is $\Delta(\delta\delta)(S,S)$ whereas in the cation studied by Marusak *et al.*[5] it is $\Delta(\delta\delta)(R,R)$. This observation suggests that the relative orientation of the NH hydrogens affects the bonding pattern between the cations, which in turn determines the choice of crystallization pathway.

The diastereoisomers present in complex **3** have an unexpected packing mode. First, Fig. 6 shows that in this substance the cations pack with their oxalate ligands pointing at each other across the inversion centre, creating pairs the members of which are diastereoisomerically related. This is obvious from the central pair inside the cell in Fig. 6. Secondly, all the cations of the upper row are Δ while those of the lower one are Λ. Thirdly, the cations form, altogether, five hydrogen bonds to amine hydrogens, as listed in Table 6; however, each of them links a given cation to five different ones. Thus, the hydrogen-bonded spiral pattern, thus far found to lead to conglomerate crystallization, is absent here also. Fourthly, lateral contacts, along the *c* axis, are between CH_2 hydrogens, which cannot hold the molecules together very strongly.

Acknowledgements

We thank the Robert A. Welch Foundation for support of this research (Grant E-592 to I. B.) and for fellowships granted to J. M. and J. C. We thank the National Science Foundation for the funds used in purchasing the diffractometer.

References

1 A. Werner, *Chem. Ber.*, 1914, **47**, 2171.
2 K. Yamanari, J. Hidaka and Y. Shimura, *Bull. Chem. Soc. Jpn.*, 1973, **46**, 3724; A. Fuyuhiro, K. Yamanari and Y. Shimura, *Bull. Chem. Soc. Jpn*, 1991, **54**, 2531.
3 R. D. Gillard and L. H. R. Tipping, *J. Chem. Soc., Dalton Trans.*, 1977, 1241.
4 I. Bernal, J. Myrczek and J. Cai, *Polyhedron*, 1993, **12**, 1149.
5 R. A. Marusak, M. A. Ivanca, K. J. Haller and A. G. Lappin, *Inorg. Chem*, 1991, **30**, 618.
6 W. T. Jordan and L. R. Froebe, *Inorg Synth.*, 1978, **18**, 96.
7 SDP-Plus, Enraf-Nonius Corporation X-ray diffraction data processing programs, distributed by B. A. Frenz & Associates, College Station, TX, 1985.
8 A. C. Larson, F. L. Lee, Y. Le Page, M. Webster, J. P. Charland and E. J. Gabe, The NRCVAX Crystal Structure System, as adapted for PC use by P. S. White, University of North Carolina, Chapel Hill, NC, 1990.
9 R. B. Roof, *A Theoretical Extension of the Reduced Cell Concept in Crystallography*, Report LA-4038, Los Alamos Scientific Laboratory, 1969.
10 D. T. Cromer and J. T. Waber, *International Tables for X-Ray Crystallography*, Kynoch Press, Birmingham, 1975, vol. 4, Tables 2.2.8 and 2.3.1.
11 J. Cai, J. Myrczek and I. Bernal, *J. Chem. Soc., Chem. Commun.*, 1992, 1147.
12 I. Bernal, J. Cetrullo, J. Myrczek and S. S. Massoud, *J. Coord. Chem.*, 1993, **30**, 29.
13 G. H. Searle and F. G. Keene, *Inorg. Chim. Acta*, 1989, **155**, 125.
14 R. N. Keller and L. J. Edwards, *J. Am. Chem. Soc.*, 1952, **74**, 215.
15 S. F. Pavkovic and D. W. Meek, *Inorg. Chem.*, 1965, **4**, 20.
16 F. Basolo, *J. Am. Chem. Soc.*, 1953, **75**, 227.
17 E. W. Gillow and G. M. Harris, *Inorg. Chem.*, 1968, **7**, 394.
18 D. A. Buckingham, L. G. Marzilli and A. M. Sargeson, *J. Am. Chem. Soc.*, 1967, **89**, 3428.
19 D. A. Buckingham, L. G. Marzilli and A. M. Sargeson, *Inorg. Chem.*, 1968, **7**, 915.
20 W. T. Robinson, D. A. Buckingham, G. Chandler, L. G. Marzilli and A. M. Sargeson, *Chem. Commun.*, 1969, 539.
21 J. A. Hearson, S. F. Mason and R. H. Seal, *J. Chem. Soc., Dalton Trans.*, 1977, 1026.
22 D. A. Buckingham, L. G. Marzilli and A. M. Sargeson, *J. Am. Chem. Soc.*, 1967, **89**, 825.
23 T. W. Hambley, C. J. Hawkins, J. Martin, J. A. Palmer and M. R. Snow, *Aust. J. Chem.*, 1981, **34**, 2505.
24 S. F. Mason, *Chem. Commun.*, 1969, 856.
25 S. F. Mason, *J. Chem. Soc. A*, 1971, 667.
26 E. J. Corey and J. C. Bailar, *J. Am. Chem. Soc.*, 1959, **81**, 2620.
27 I. Bernal, J. Cetrullo, J. Myrczek, J. Cai and W. T. Jordan, *J. Chem. Soc., Dalton Trans*, 1993, 1771.
28 I. Bernal, J. Cai and J. Myrczek, *Acta Chim. Hung.*, 1993, **130**, 555.
29 I. Bernal and J. Cetrullo, *Inorg. Chim. Acta*, 1986, **120**, 109.

Received 22nd *July* 1994; *Paper* 4/04488F